Comparisons of Cloud Cover Estimates and Cloud Fraction Profiles from ARM's Cloud-Detecting Instruments and GOES-8 Data

D.J. Rodriguez
S.K. Krueger

This paper was prepared for submittal to the

First International Symposium on Turbulence and Shear Flow Phenomena
Santa Barbara, CA
September 12-15, 1999

May 7, 1999

Comparisons of Cloud Cover Estimates and Cloud Fraction Profiles from ARM's Cloud-Detecting Instruments and GOES-8 Data

Daniel J. Rodriguez
Atmospheric Science Division
Lawrence Livermore National Laboratory
Livermore, CA

Steven K. Krueger
Department of Meteorology
University of Utah
Salt Lake City, UT

Introduction

The DOE's Atmospheric Radiation Measurement (ARM) Program employs both upward- and downward-looking remote-sensing instruments to measure the horizontal and vertical distributions of clouds across its Southern Great Plains (SGP) site. No single instrument is capable of completely determining these distributions over the scales of interest to ARM's Single Column Modeling (SCM) and Instantaneous Radiative Flux (IRF) groups; these groups embody the primary strategies through which ARM expects to achieve its objectives of developing and testing cloud formation parameterizations (USDOE, 1996). Collectively, however, the data from ARM's cloud-detecting instruments offer the potential for such a three-dimensional characterization. Data intercomparisons, like the ones illustrated in this paper, are steps in this direction. Examples of some initial comparisons, involving satellite, millimeter cloud radar, whole sky imager and ceilometer data, are provided herein.

Data Intercomparisons

The variety of instrumentation is greatest at the SGP Central Facility (CF). Given that more opportunities for data intercomparison exist at the CF, our attention has been mainly focused there with the expectation that many of the lessons learned can later be adapted to cloud data at the Boundary and Extended Facilities. Principally, we are concerned about: 1) the accuracy of various estimates of cloud properties at a single point, or within a thin vertical column, above the CF over time, and 2) the accuracy of various estimates of cloud properties over the Cloud and Radiation Testbed (CART) site, which can then be reduced to single, representative profiles over time. In the former case, the results are usable in the IRF and SCM strategies; in the latter case, they satisfy SCM needs specifically.

The Whole Sky Imager (WSI) and ceilometer data used in one study were collected at the SGP CF between October 1 and December 31, 1996 (Shields, et. al., 1990). This three-month period, corresponding to the first set of WSI data released by ARM's Experiment Center, was sufficiently long to reveal important trends (Rodriguez, 1998). Comparisons were made by invoking the ergodic assumption, whereby ensemble, time and space averages are assumed to be equivalent. Hourly values of cloud fraction from WSI data were formed by averaging cloud cover estimates, derived from pixel values within a 10-degrees-of-zenith area, from six 10-minute images. A corresponding ceilometer estimate

was formed by dividing the cloud detections by the total number of measurements, typically 60, over the same hour. Use of either the Micropulse Lidar (MPL) or Belfort Laser Ceilometer (BLC) data in defining the cloud occurrence frequency (COF) over an hour's time depended on the cloud base height; it is generally acknowledged that the BLC is best at detecting clouds in the 0-3000 m range, while the MPL has greater sensitivity at higher altitudes (Turner, 1990; Spinhirne, et. al., 1995).

The scatter of points in Fig. 1, based on temporal pairings of the WSI and ceilometer cloud fractions, reveals the relationship between these data. In particular, the points aligned along the ordinate, which correspond to clear (WSI) and varying cloudy (ceilometer) combinations, show the poor correlation between these paired-in-time data. Inspection of many associated data records confirms that the WSI algorithm often produces cloud fraction estimates of zero, while the MPL, with its greater sensitivity, reports the presence of thin or sub-visual cirrus. (Biases to this degree should diminish with the new WSI daytime algorithm.) The correspondence between the hourly WSI and ceilometer comparisons decays with increasing cloud base height until it becomes uncorrelated at 5000 m and beyond.

Cloud amounts over ARM's Central Facility, based on measurements of radiance by NASA's Geostationary Operational Environmental Satellite (GOES-8) radiometer and analyses by the Langley Research Center on a 3x3 grid, are compared against hourly, time-centered COFs derived from MPL data in Fig. 2 (Minnis and Smith, 1998). The time line, expressed in Julian days, spans the July 1995 SCM IOP, which the SCM group refers to as Case 1. The more darkly shaded areas correspond to times at which the satellite estimates exceed the MPL estimates; the lightly shaded areas represent the converse situation. Overall, the agreement is good, but the darkly shaded areas dominate the scene. Analyses of the satellite data suggest that the skies tend to be clear or overcast, while detections by the MPL suggest a higher frequency of scattered and broken clouds. Possible reasons for these discrepancies will be explored momentarily.

One way of quantifying the biases noted in the Fig. 2 is to calculate and compare the time-mean cloud amounts from the satellite and MPL data over the July 1995 SCM IOP. Occasionally, one or both instruments were inoperative, leading to averages composed of as few as 15 values and as many as 23 values. The results in Fig. 3 split naturally into two groups. During the nighttime, the cloud cover estimates from MPL data generally exceed the estimates from satellite data, but only slightly; conversely, during the daytime, the GOES-8 estimates always exceed the MPL estimates by a sizable amount. Both sets of curves track one another reasonably well, suggesting that the same cloud fields are being observed, but interpreted somewhat differently.

Thus far, three plausible explanations for these results have surfaced, none of which are necessarily exclusive or correct. One obvious explanation would be that the signal returned to the MPL receiver was severely affected by solar contamination. However, the outcome of the WSI and ceilometer data comparisons would suggest otherwise. Next, upon checking with the designers and builders of the MPL, we discovered that in July 1995 the laser was operating at half its current power of 1 W, meaning that the return signal was about an order of magnitude less than its current strength. In other words high, optically thin clouds may have escaped detection by the MPL, leading to under-estimations of cloud amount. Lastly, the bi-spectral (0.63 and 11 micron) threshold technique being applied to the GOES-8 radiance data during the daytime may tend to over-represent cloudiness due, perhaps, to difficulties in specifying clear sky radiances..

For Case 1, the satellite product used is based on radiance data collected within a 0.3 ° box, centered over the CF and comprised of approximately 60 pixels. The pixels are either clear or overcast depending on thresholds determined as functions of scene type, solar and satellite viewing angles, and

clear sky radiances. The cloud amount is simply the fraction of overcast pixels within the grid box. For purposes of comparison, we "mimicked" the satellite data, using MPL data, in accordance with the following arguments. If the pixel resolution is dx and the mean wind speed at cloud height is u, then a pixel will traverse the MPL sampling space in time interval dt = dx/u. If the mean wind speed is 10 m/s, a "conservative" cloud element travels 40 km, or roughly $0.3°$, in about one hour. If, as in the previous analyses, we retain the 1-hour window for the MPL data, centered on the satellite observation time, and if we assume that the MPL "pixels" are 4 km wide, corresponding to the pixel resolution of the GOES-8 radiometer, there will be 10 cloud characterizations per hour, i.e., dt will equal 6 minutes. While the resulting resolution is admittedly coarse (cloud amounts over an hour's time are multiples of 10% for MPL data averaged over one minute), the characterizations are not believed to be overly restrictive when diurnal composites are formed over 24 days.

With these conditions and assumptions in effect, we defined an MPL "pixel" as being overcast in three different ways:

  1. A cloud is detected by the MPL at least once during time interval dt;
  2. Clouds are detected at least half the time during time interval dt; and
  3. Clouds are always present during time interval dt.

The curves and points labeled thresh_1, thresh_half and thresh_all in Fig. 4 correspond, respectively, to cloud definitions 1, 2 and 3 above. During the daytime, thresh_1 is best at matching the diurnally-averaged satellite cloud amounts, while during the nighttime the thresh_all definition is best. The nighttime result may indicate that the IR threshold scheme in use at the time of the analyses had difficulty distinguishing low cloud tops from the ground surface. Lastly, a comparison of these results against the time series of MPL and GOES-8 cloud amounts in Fig. 2 suggests that the apparent

overestimation in the frequency of overcast conditions, as derived from satellite data, occurred during periods of scattered and broken clouds, as registered by the lidar.

Representative profiles of cloud fractions over time at the SGP site are valued by the SCM group as they provide important statistics against which a particular set of model results can be compared. The data stream from which this product has been derived resides in the $0.5°$ GOES-8 file. It contains cloud amounts, cloud top heights and cloud thicknesses at levels that correspond to low (< 2000 m), middle (2000–6000 m) and high (> 6000 m) cloud layers on a 20x28 grid. Using a 5x5 subset of the $0.5°$ cloud amounts, whose area approximately matches the horizontal dimension of an SCM column, 25 individual profiles of cloud occurrence were constructed at regular, vertical (250 m) intervals up to 15 km by assigning a value of one to grid points within a cloud and a value of zero to those without, and by multiplying the profile values within the cloud layers by the appropriate cloud amounts. Cloud amounts were then averaged at each vertical grid level. These steps were repeated for each new data time and were followed, if necessary, by linear interpolations every two hours. The resulting time-height arrays of cloud fractions (our definition excludes overlap assumptions) were then contoured and color-filled. The results of this exercise for the second half of the Summer 1997 SCM IOP, also known as SCM Case 3, are shown in Fig. 5. The absence of cloud thickness analyses precludes plotting during the nighttime (the first half of each Julian day).

Similar, but less complicated, procedures were used in deriving cloud fractions for the MMCR data, as shown in Fig. 6. The MMCR data records are more intact, giving us a nearly continuous view of cloudiness over the Central Facility. The smoothing effects of spatial averaging are evident in the previous figure; in contrast, the gradients between clear and cloudy skies in the MMCR plot are much sharper. Generally, though, the picture that emerges when comparing Figs. 5 and 6 is fairly consistent.

Both instruments show the presence of clouds at about the same time, and cloud top heights are comparable; however, the heights of cloud bases rarely agree. There are several possible reasons. The downward-sensing radiometer cannot discriminate between single- and multi-layer clouds, i.e., the instrument measures the composite effects of radiating clouds along a viewing path, so there may be a tendency for overestimating the lowest cloud-base height. On the other hand, the signal from the upward-sensing MMCR is susceptible to contamination by insects and precipitation, i.e., the shafts that reach the ground in Fig. 6 are indicative of a rain event or insects in the boundary layer, both of which can severely attenuate the radar signal and mask the true cloud base. Other researchers have employed more rigorous, value-added procedures for identifying cloud boundaries than we used here.

Discussion

Collecting measurements at the SGP and other ARM sites over long periods of time and for a variety of weather conditions is critical to the formation and testing of parameterizations for GCMs, a primary programmatic objective of ARM. The principal means of collecting cloud data, which supports one aspect of this objective, is by remote sensing. Often, measurements and products derived from these measurements provide a unique, if uncertain, resource; for example, the estimation of some cloud macrophysical features across the CART site, as offered by NASA Langley's analyses of satellite radiance data, is comprehensive in its horizontal coverage, but it remains to be seen whether their cloud height analyses are sufficiently and routinely accurate for purposes of model testing. Other instruments, like the millimeter-wavelength cloud radar in combination with ceilometers, use active sensing to penetrate clouds and provide information on their heights and structures, but only in an atmospheric column directly above the radar, i.e., the sampling volume lacks the breadth of spatial coverage that instruments, like satellite-mounted radiometers, can offer. Over time, best-estimate data and data products will emerge from investigations like the ones described here.

References

Minnis. P., and Smith, W.L., Jr.: Cloud and Radiative Fields Derived from GOES-8 During SUCCESS and the ARM-UAV Spring 1996 Flight Series, *Geophys. Res. Ltrs.*, 25, April 15, 1998, pp. 1113-1116.

Rodriguez, D.J., 1998: On the Comparability of Cloud Fractions Derived from Whole Sky Imager and Ceilometer Data, Lawrence Livermore National Laboratory Report UCRL-ID-129829.

Shields, J.E. T.L. Koehler, M.E. Karr and R.W. Johnson, 1990: Automated Cloud Cover and Visibility Systems for Real Time Applications. University of California, San Diego, Scripps Institution of Oceanography, Marine Physical Laboratory, Optical Systems Group Technical Note No. 217.

Spinhirne, J.D. J.A.R. Rall, and V.S. Scott, 1995: Compact Eye Safe Lidar Systems, *Rev. Laser Eng.*, 23, 112-118..

Turner, D.D., 1996: Comparisons of the Micropulse Lidar and the Belfort Laser Ceilometer at the Atmospheric Radiation Measurement Southern Great Plains Cloud and Radiation Testbed Site, Proceedings of the Sixth Atmospheric Radiation Measurement (ARM) Science Team Meeting, San Antonio, Texas, 4-7 March. U.S. Department of Energy, Washington, D.C.

United States Department of Energy, 1996: Science Plan for the Atmospheric Radiation Measurement Program (ARM), DOE/ER-0670T, Washington, D.C
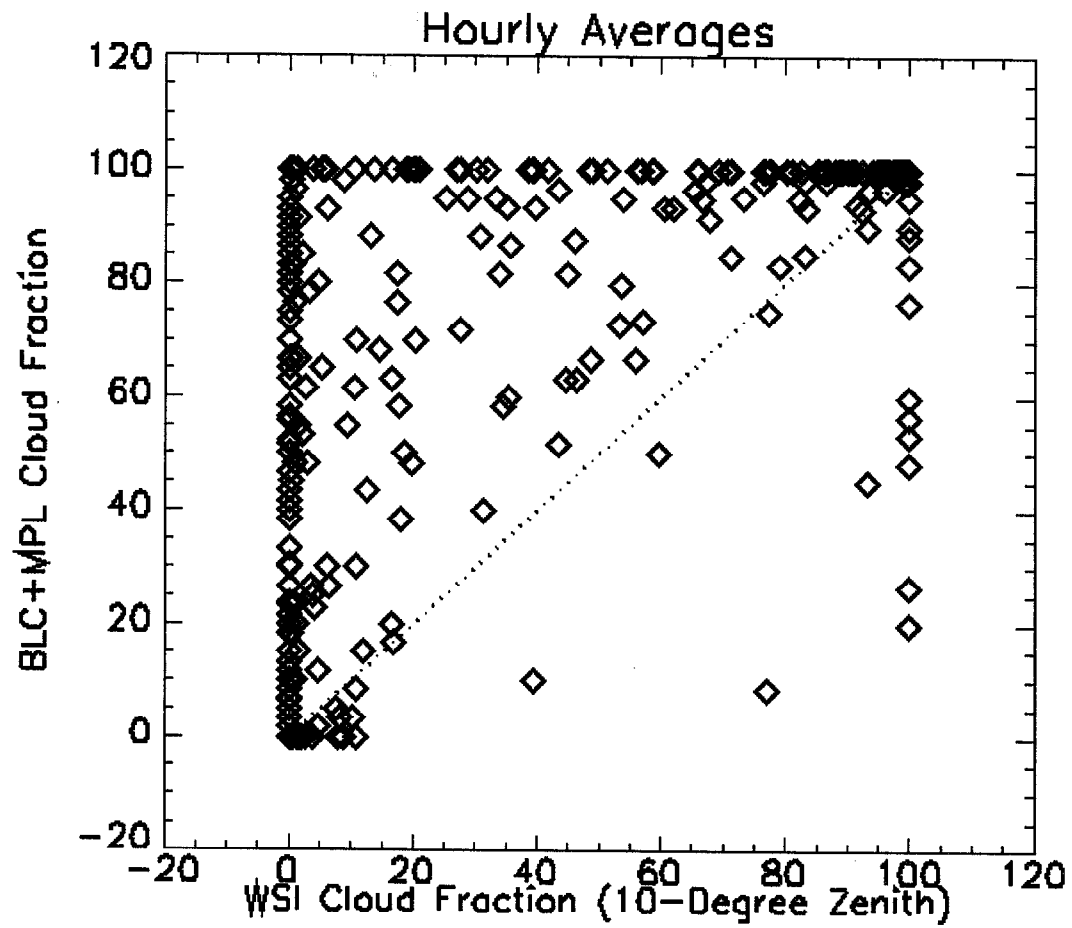
Figure 1. Scatter plot of the hourly, paired-in-time cloud fractions from the 10 ° WSI and merged BLC and MPL data at the SGP Central Facility over the Fall months of 1996.
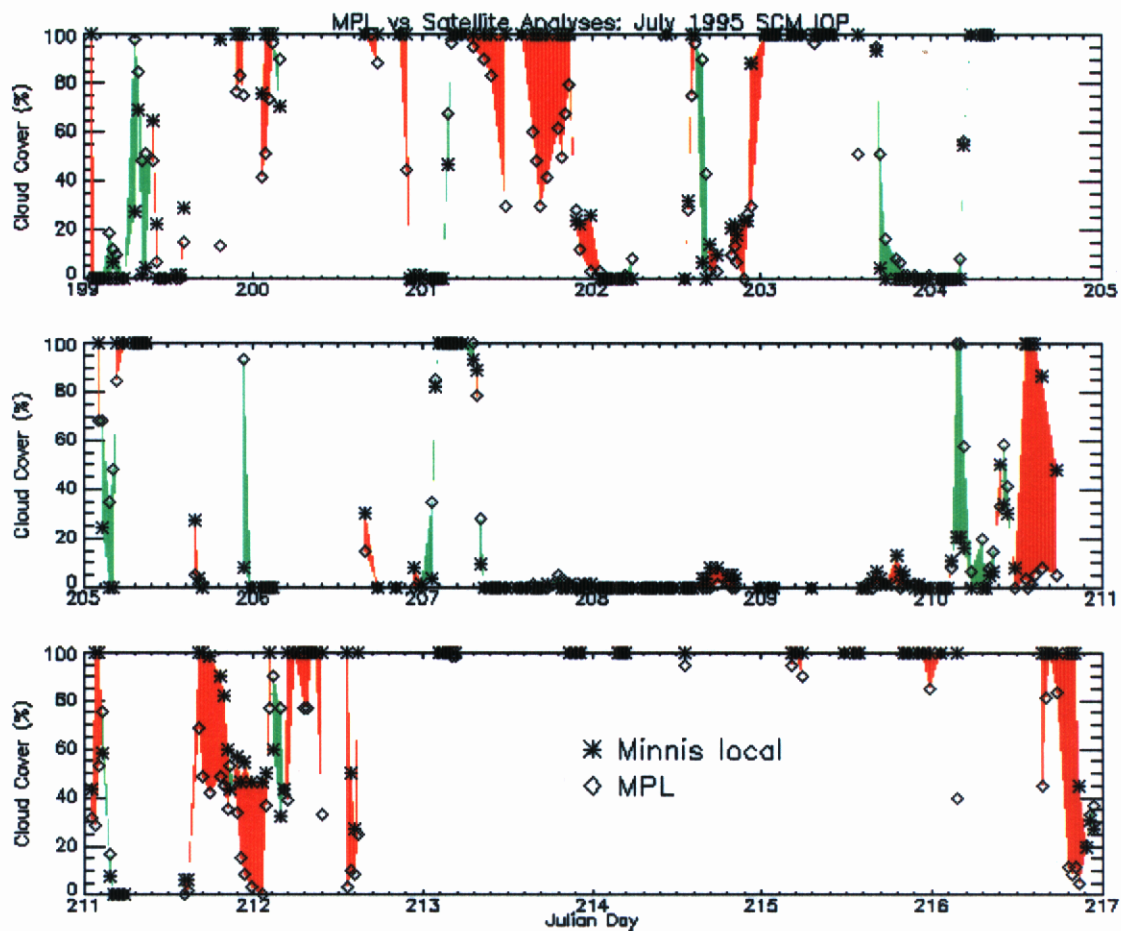
Figure 2. Comparison of cloud covers from the Minnis analyses of GOES-8 0.3 $^\circ$ (~ 60 pixels) radiance data over the SGP CF and cloud occurrence frequencies from the MPL time-centered, hourly-averaged data during the July 1995 SCM IOP.
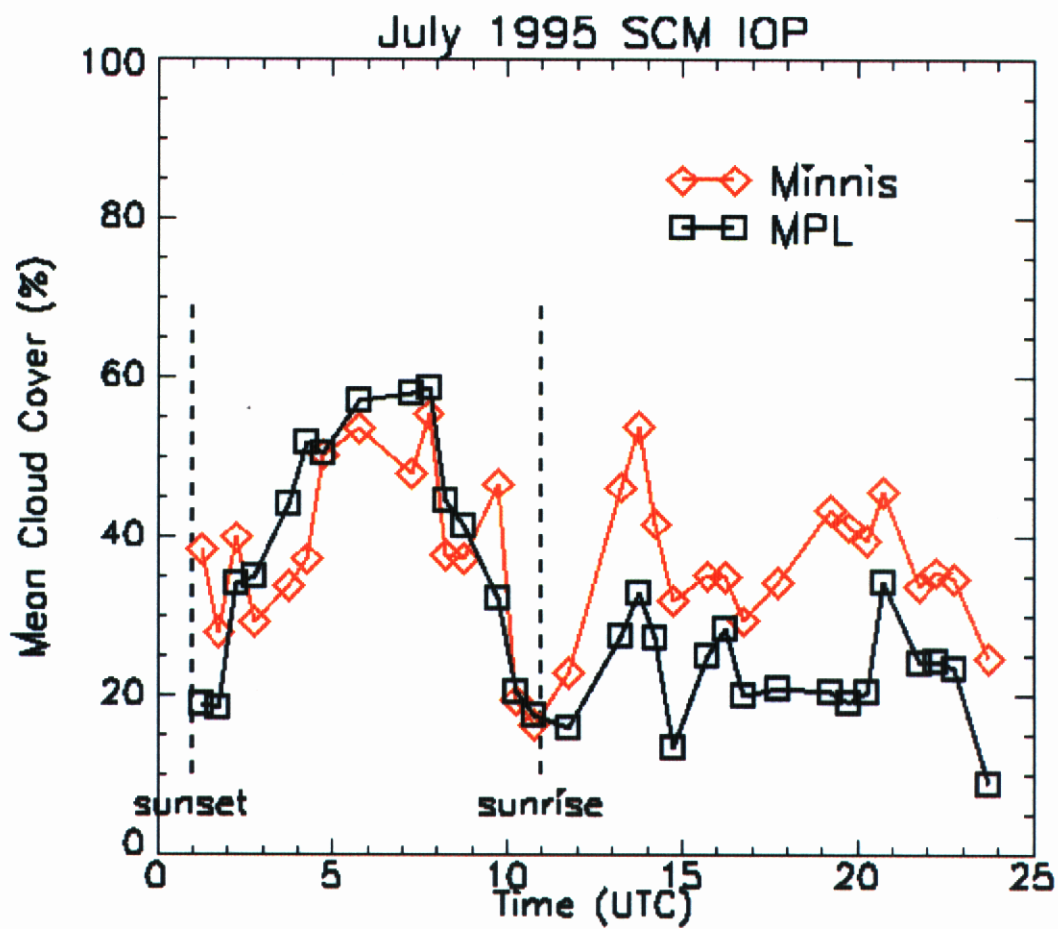
Figure 3. Diurnal composites of cloud amounts over the SGP CF as estimated from MPL and Minnis local (0.3 °) satellite data during the July 1995 SCM IOP.
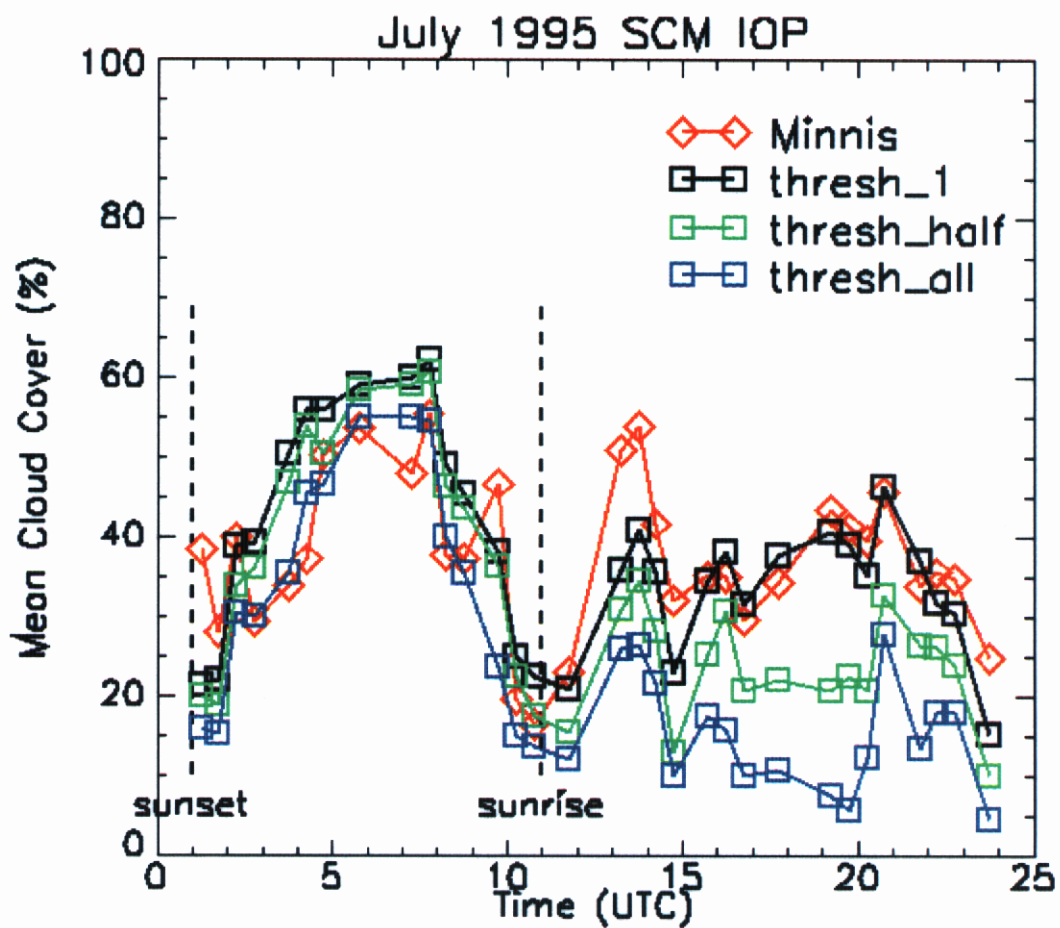
Figure 4. Diurnal cloud amounts over the SGP CF based on local GOES-8 and MPL "pixel" data from the July 1995 SCM IOP.
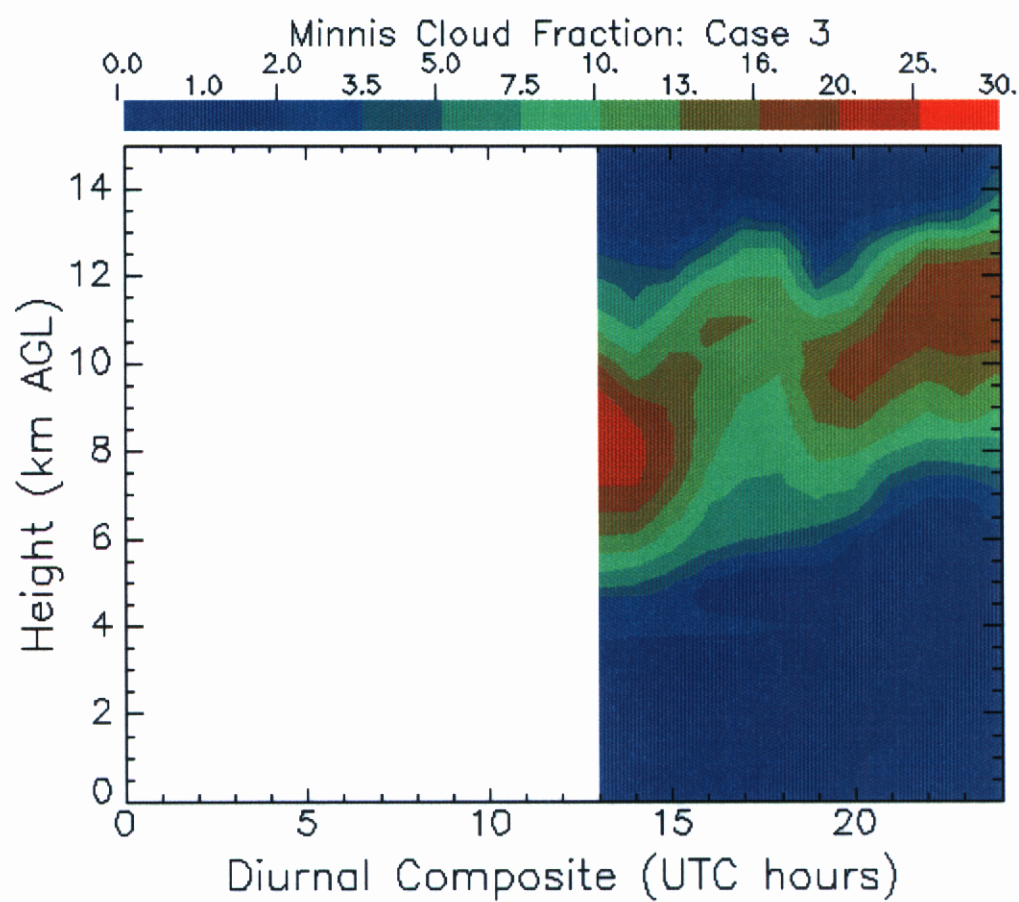
Figure 5. Cloud fraction derived from satellite cloud layer analyses, averaged by time of day over the entire CART site during the Summer 1997 SCM IOP.
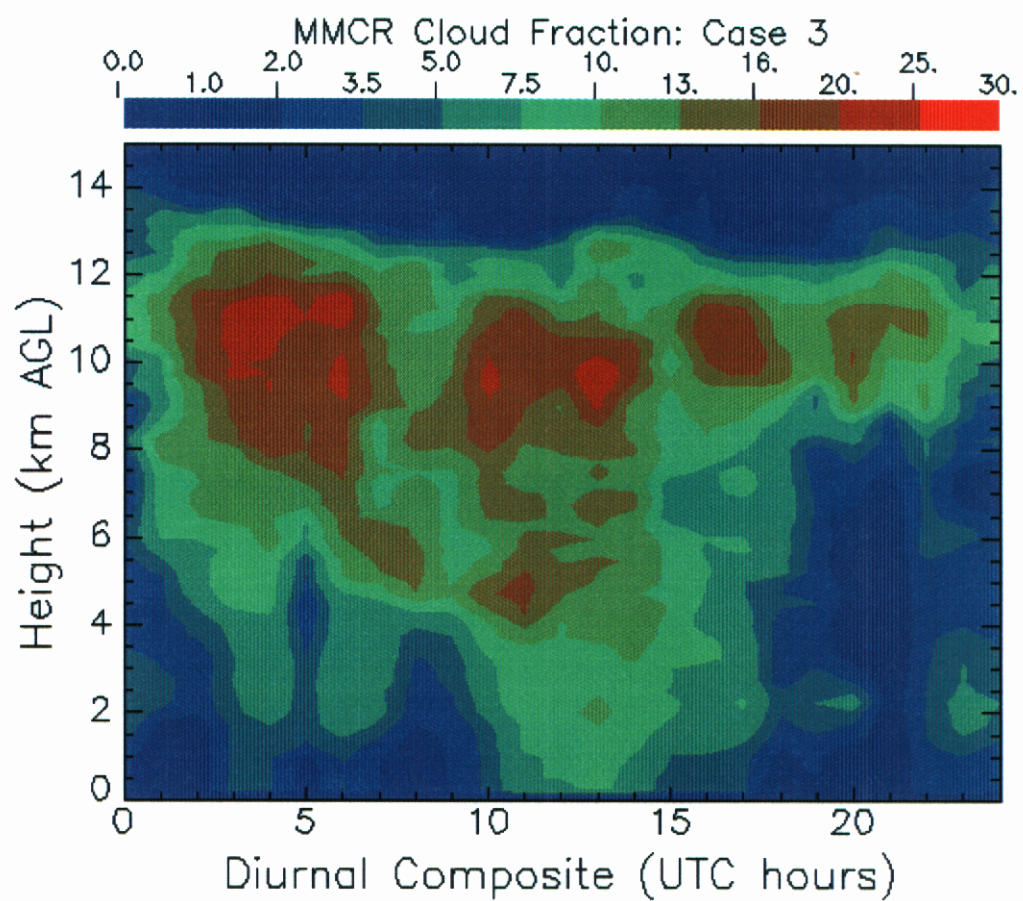
Figure 6. Cloud fractions derived from MMCR cloud occurrence frequencies during the Case 3 SCM IOP.